

Faint M-dwarfs and the structure of the Galactic disk ¹

I. N. Reid, J. E. Gizis, J. G. Cohen, M. A. Pahre

Palomar Observatory, 105-24, California Institute of Technology, Pasadena, CA 91125,
e-mail: inr@astro.caltech.edu, jeg@astro.caltech.edu, jlc@astro.caltech.edu,
map@astro.caltech.edu

D. W. Hogg

Theoretical Astrophysics, 130-33, California Institute of Technology, Pasadena, CA 91125,
e-mail: hogg@tapir.caltech.edu

L. Cowie, E. Hu, A. Songaila

Institute for Astronomy, University of Hawaii, 2680 Woodlawn Drive, Honolulu, HI 96822,
e-mail: cowie@ifa.hawaii.edu, acowie@ifa.hawaii.edu, hu@ifa.hawaii.edu

ABSTRACT

We use broadband photometry and low-resolution spectra of a complete sample of late-K and M dwarfs brighter than $I=22$ in three fields at high galactic latitude to study issues relating to galactic structure and large scale abundance gradients in the Galaxy. The observed starcounts in each field are a good match to the predictions of models based on deep starcount data in other intermediate-latitude fields, and these models identify the late-type stars as members of the Galactic disk. Abundances for these late type stars are estimated via narrowband indices that measure the strength of the TiO and CaH bands in their spectra. Our results show that the average abundance in the Galactic disk remains close to solar even at heights of more than 2 kpc above the Plane.

Subject headings: stars: late type, Galaxy: Abundances, Galaxy: Structure

¹Based partly on observations obtained at the W.M. Keck Observatory, which is operated jointly by the California Institute of Technology and the University of California, partly on data from the 200-inch telescope at Palomar mountain, owned and operated by the California Institute of Technology, and partly on data from the 60-inch telescope at Palomar Mountain which is jointly owned by the California Institute of Technology and the Carnegie Institution of Washington

1. Introduction

It is by now generally agreed that the vertical distribution of stars in the Galactic disk cannot be represented by a simple, single-component density law. Deep, wide-field optical number-magnitude starcounts show that the slope of the overall density distribution flattens by a factor of ~ 4 between 1.2 and 1.5 kiloparsecs above the Plane, well before the halo becomes the dominant population at $z \sim 5$ kpc (Gilmore & Reid, 1983; Majewski, 1992; Reid & Majewski, 1993 - hereinafter, RM93; Gould, Flynn & Bahcall, 1996). What is not clear, however, is how one interprets these ‘extra’ stars, both in terms of deconvolving the observed distribution into thin and thicker components (Majewski, 1993; Robin, 1994) and in deciding the physical significance of the deconvolved components.

Majewski (1993) outlines eight different scenarios for the formation of what we will refer to as the intermediate population (or IP II), and one can characterise the extremes as being those models which treat the IP II as the result of a separate, distinct star formation event (e.g. Wyse & Gilmore, 1988; Robin et al, 1996) and those which identify the IP II as the high-velocity tail of the old disk (Norris, 1987). One method of constraining these various hypotheses is through measurement of the abundance distribution of the stars in the IP II, in particular determining whether there is a significant gradient in the mean abundance with height above the Galactic Plane. To date, however, the requisite observational data are still relatively sparse. Yoss, Neese & Hartkopf (1987) use observations of high-latitude K-giants to derive a metallicity gradient of ~ -0.4 dex kpc $^{-1}$ to $z=700$ pc. and ~ -0.18 dex kpc $^{-1}$ thereafter (to 8 kpc), although their sample includes relatively few stars above 2.2 kpc and shows substantial dispersion. Trefzger, Pel and Gabi (1995) and Gilmore, Wyse & Jones (1995) have surveyed F and G dwarfs towards the South Galactic Pole, using VBLUW photometry and medium resolution, low signal-to-noise spectra respectively. Again, neither study include many stars above 2.5 kiloparsecs. Trefzger et al find a relatively steep gradient close to the Plane (~ -0.55 dex kpc $^{-1}$), and both match the K giant survey in finding little variation in the mean abundance above ~ 1 kiloparsec, although Gilmore et al’s data show significantly more dispersion. Finally, Majewski’s (1992) UBV data extend to $z > 10$ kpc and suggest a somewhat higher mean abundance below 6 kiloparsecs.

In this paper we present the first attempt to use observations of distant late-type K and M dwarfs to study this question. At least 80 % of the stars in the Galactic disk are M dwarfs, so these stars have a high surface density at faint magnitudes. Moreover M dwarfs can be recognized even with low dispersion spectra. At the faint magnitude level under consideration, any M star seen must be an M dwarf; high luminosity M giants and supergiants would be so far out in the galactic halo that even if they were to be found there in the same ratio as K giants and K supergiants (which is unlikely given the higher

metallicity required to produce M giants), their surface density would be insignificant compared to the number of bona fide M dwarfs.

Furthermore low-abundance M-type subdwarfs can be identified through the enhanced strength of the hydride bands (particularly CaH) relative to the TiO absorption (Bessell, 1982). Until recently, the complex, diatomic-molecule dominated spectra of these stars defied quantitative abundance analysis, but Gizis (1997) has shown that the atmosphere models developed by Allard & Hauschildt (1995) can be combined with narrowband spectrophotometry to derive an approximate ($\sim \pm 0.3$ dex) abundance scale for these stars. Given these results, we have undertaken a preliminary study, analysing Keck LRIS data of a magnitude-limited sample of faint M-dwarfs. Section 2 describes the observational data; section 3 compares the observed colour-magnitude diagrams against Galactic starcount models and discusses the abundance distribution; section 4 summarises our conclusions.

2. Observations

Our sample consists of the K and M dwarfs drawn from three fields: the 0-hour deep field ($l=125^\circ$, $b=-50^\circ$); SSA 13 ($l=109^\circ$, $b=74^\circ$); and SSA 22 ($l=63^\circ$, $b=-44^\circ$). The first field is 7.3×2 arcminutes in size (0.004 square degrees), while the other two fields are $6' \times 2'$ (0.003 sq. deg.). All three fields are part of a deep, K-band limited redshift survey being undertaken by groups at Caltech (Cohen et al, 1996) and Hawaii (Cowie et al, 1996). The primary goal is a deep redshift survey of extragalactic objects, but objects within the magnitude limits were observed irrespective of morphology. Here we concern ourselves with the galactic stars found during the course of these redshift surveys. This paper discusses observations of the complete sample of 68 stars with $I < 22$ mag. in these fields.

The spectroscopic sample consists of those objects with observed spectra judged to have sufficient signal-to-noise ratios to be useful in deducing abundances for these K and M dwarfs. It includes 43 stars. The spectroscopic observations of the 0 hour field sources are described in detail by Cohen et al (1997), while Cowie et al (1996) discuss the data for objects in the two Hawaii fields.

A detailed description of the observations and analysis of the U, B, V, R, I , and K photometry for the 14 stars in the 0 hour field can be found in Pahre et al (1997). The same can be found for the Hawaii fields (observed only at B, I , and K) in Cowie et al (1996). We have supplemented the SSA22 data with BVI photometry obtained with LRIS on the Keck telescope in September, 1996, calibrating the observations using the same methods outlined by Pahre et al (1997). These observations included shorter-exposure images, and hence

avoided saturating the brighter stars. We have used the IRAS 100 μm maps to estimate the interstellar absorption in each field. Using the calibration given by Laureijs, Helou & Clark (1994), we estimate a total extinction of $A_V \sim 0.22$ mag in the 0-hour field, corresponding to $A_I \sim 0.10$, $E_{B-I} \sim 0.19$ and $E_{I-K} \sim 0.08$ mag; $A_V \sim 0.23$ mag in SSA22; and negligible extinction ($A_V \sim 0.005$ mag) in SSA13. We assume that all of the extinction lies in the immediate vicinity (within 200 pc.) of the Sun. Figure 1 shows the reddening-corrected two-colour $(B - I)/(I - K)$ diagram for all of the spectroscopically-confirmed stars in these fields.

All of the objects were observed spectroscopically using multislit masks with LRIS (Oke et al, 1994) on the Keck 10-metre telescope. The slits used were 1.4 arcseconds wide, and a 300 l/mm grating gives spectra of 16 \AA (~ 5 pixels) resolution covering the wavelength range ~ 5000 to 10000 \AA . (The actual coverage on each spectrum depends on the exact position of the slit within the rectangular field.) Full details of the reduction procedures are given in Cowie et al (1996) and in Cohen et al (1997). The spectra from the 0 hour field were set on a flux scale using observations of the white dwarf standard G191-B2B (Oke 1990). This star was observed using a 1.5 arc-sec aperture longslit in LRIS. While the calibration takes out the overall spectral response of the CCD, varying losses of light at the slit lead to the calibrations for individual multi-slits being uncertain by up to 10 % over broad wavelength intervals of $\sim 2000\text{\AA}$ or more. However, the widest of our narrowband indices spans only 250 \AA , so the uncertainties in the indices are dominated by the signal-to-noise in the individual spectra rather than by systematic errors in the flux calibration.

3. Discussion

3.1. Starcounts

We have compared the observed colour-magnitude distribution of the photometric sample of sixty-eight stars with $I < 22$ mag. against the predictions of starcount models. As the starting point for our analysis, we take model B from Reid *et al* (1996 - hereinafter RYMTS). This model includes three stellar components: the old disk, modelled as a $\text{sech}^2 \frac{h}{h_0}$ distribution, with h_0 of 350 parsecs; an intermediate population, with a local normalisation of 5 % relative to the old disk and a sech^2 density law, $h_0 = 1500$ pc.; and an $r^{-3.5}$ halo with the local density normalised to 0.15 % that of the old disk. We have also adopted a scalelength of 2.5 kiloparsecs for the radial density law in the Galactic disk (Robin, Cr ez e & Mohan, 1992). The colour-magnitude relations adopted for these three populations are from photometry of nearby stars, of members of the open cluster NGC 2420 and of stars in the globular cluster NGC 6752, respectively. Full details are given in RYMTS, who show that

this model reproduces both the colour-magnitude distribution in the intermediate-latitude PSR 1640 field ($l=41^\circ$, $b=38^\circ$) and the density distribution towards the South Galactic Pole.

Figure 2a compares the overall starcount predictions of model B against the observations in the three fields considered in this paper. The agreement is well within the formal Poissonian uncertainties. Limiting the sample to the magnitude range $17 < I < 22$, we observe 19, 11 and 37 stars in the 0 hour field, SSA13 and SSA22. The predicted numbercounts are 15, 11 and 32 stars in the respective fields.

Figure 2b compares the colour-magnitude distributions predicted by this model against the observed (I, (I-K)) distribution in each field. For greater clarity, the predicted starcounts in each field are matched to a solid angle of 0.01 square degrees - a factor of 2.5 greater than the 0-hour field and ~ 3 greater than the SSA 13 and SSA 22. The model predicts two distinct sequences: late F- and G-type halo subdwarfs ($(I-K) < 1.5$) lying at a distance of ~ 10 kiloparsecs; and a sequence of late-K and M-type disk dwarfs, mainly contributed by the IP II, at distances of from ~ 1 to 4 kiloparsecs. The small scaleheight of the old disk component leads to a low surface density and an insignificant contribution to these faint starcounts, even in the intermediate-latitude field SSA22.

As described in RYMTS, the convolution of the density law and the sampling volume lead to a preferred distance modulus for a given stellar population. Since the old disk has the steepest vertical density law and the halo the shallowest, the former stars are sampled primarily at $(m-M) \sim 7$ magnitudes, while the latter lie preferentially at $(m-M) \sim 15$ magnitudes. Thus, at a given apparent magnitude, the halo contributes more luminous (bluer) stars than the disk. The models plotted in figure 2b clearly show that the later-type stars, which contribute the bulk of the stars in each field, are members of the Galactic disk.

3.2. The abundance distribution

The primary aim of this paper is to use the late-type dwarfs in our sample to probe the abundance distribution at large distances above the Plane. In order to do this we need to estimate both abundances and distances. We have used B-, I- and K-band data for individual stars within 8 parsecs to define $(M_I, (B-I))$ and $(M_I, (I-K))$ relations (figure 3). The curves fitted are sixth order polynomials, and the dispersion is $\sigma_I = 0.35$ magnitudes in the (B-I) calibration and $\sigma_I = 0.52$ magnitudes for (I-K). Comparing the distance estimates for individual stars, the mean difference between the (B-I) and (I-K) photometric parallaxes is 40 % of the distance based on averaging the two estimates, with no evidence

of a systematic offset between the two distance scales. We have therefore taken the straight average of the two estimates as the appropriate distance for each star and adopt an uncertainty of $\sim 30\%$. This is adequate for the present purposes.

Gizis (1997) has shown that abundance estimates for late-K and M-type dwarfs can be derived from the relative strengths of the calcium hydride band at $\sim 6800\text{\AA}$ and the titanium oxide $\gamma(0,0)$ band at $\sim 7050\text{\AA}$. Reid, Hawley & Gizis (1995 - RHG) have defined several narrowband indices designed to measure the strengths of these bands, and figure 4 plots data for two of the CaH indices against TiO5, the full depth of the TiO bandhead. In addition to data (from RHG) for single disk stars within 8 parsecs of the Sun, we have plotted Gizis' measurements of the band-strength in intermediate and extreme subdwarfs. A comparison with the Allard and Hauschildt models shows that the former stars, plotted as solid square in figure 4, have an abundance of $[Fe/H] \sim -1$ while the latter are significantly more metal-poor, with $[Fe/H] \sim -2$. We have taken nearby K and M dwarfs to be representative of a solar-abundance population.

We have fitted second-order polynomials to each of the three sets of stars in figure 4 and used these as a grid to match against narrowband indices derived from our observations of the faint programme stars. Table 1 lists the band-strength data for the later-type stars in the current sample. Broadband photometry and positions for stars in SSA 13 and SSA 22 are given by Cowie et al (1996), while Pahre et al (1997) present UBVRIK for stars in the 0-hour field. Figure 5 plots the resulting bandstrengths and it is clear that the IP II stars in our sample lie closest to the polynomial fit to the local (solar abundance) stars, consistent with previous observations of IP II F and G dwarfs. We have attempted to set our abundance estimates onto a more quantitative scale by using the $[Fe/H]=0$ (nearby stars) and $[Fe/H]=-1$ (intermediate subdwarfs) sequences as fiducial references. Defining CaH^0 and CaH^{-1} as the values predicted by the solar and $[Fe/H]=-1$ relations for a given bandstrength, TiO5, we calculate the quantity

$$\Delta_C = \frac{CaH^{obs} - CaH^0}{CaH^0 - CaH^{-1}}$$

where CaH^{obs} is the observed strength of the CaH feature for the star in question. This scaling compensates for the changing separations of the two fiducial sequences, although without an adequate number of calibrators with high-precision abundance measurements, we can only assume that the variation in Δ_C with $[Fe/H]$ is similar throughout the full temperature range covered here.

Using the distances derived from the average of the photometric parallaxes, we have computed the distance, z , above the Galactic Plane for each star. Limiting the sample to

stars with significant TiO absorption ($\text{TiO5} < 0.85$), figure 6 plots the scaled CaH indices against z . The average values of the two indices if we include all stars are $\Delta_{c2} = -0.16$ and $\Delta_{c3} = -0.06$ (24 stars), while we derive $\Delta_{c2} = -0.27$ and $\Delta_{c3} = -0.06$ for the 15 stars with $z < 2000$ parsecs. As yet, we do not have sufficient calibrating observations of stars of known abundance to be able to transform these measured offsets into real abundances, but the present results are clearly suggestive of values closer to those of the old disk than previously suggested.

4. Conclusions

We have analysed photometry and low-resolution spectroscopy of faint late-K and early M-dwarfs in three intermediate- and high-latitude fields. A comparison with the predictions of a starcount model which matches the faint ($R < 24$) stellar colour-magnitude distribution in two other fields (Reid et al, 1996) shows that these stars, lying at distances of up to 2 kiloparsecs above the Plane and members of the intermediate population. Our analysis, based on the strength of CaH and TiO molecular bands, demonstrates that these stars have abundances close to that of the old disk. Clearly, these results are preliminary, both given the total number of stars in our sample and the approximate nature of the calibration of the measured bandstrength against real abundances. However, our analysis does indicate a possible new direction that can be taken in exploring the abundance distribution within Galactic stellar populations.

The Keck telescope project was made possible by a generous grant from the W.M. Keck Foundation. INR's contribution to this research was supported partially by NSF grant AST-9412463; MAP was supported by NSF award AST-9157412 and the Bressler Foundation; DWH was supported by NSF award AST-9529170.

Table 1. Spectroscopic indices

Star	TiO5	CaH2	CaH3
0 hour field			
PD0K 03	0.765	0.604	0.816
PD0K 04	0.792	0.627	0.837
PD0K 09	0.550	0.494	0.763
PD0K 16	0.643	0.503	0.790
PD0K 19	0.597	0.597	0.811
PD0K 21	0.458	0.428	0.726
PD0K 22	0.549	0.444	0.712
PD0K 49	0.387	0.419	0.693
PD0K 50	0.625	0.626	1.003
PD0K 91	0.549	0.479	0.718
PD0K 97	0.333	0.348	0.594
PD0K 101	0.392	0.597	0.689
SSA 13			
17	0.461	0.433	0.697
35	0.435	0.347	0.655
73	0.417	0.508	0.808
84	0.378	0.321	0.583
97	0.583	0.466	0.709
SSA 22			
24	0.290	0.333	0.387
61	0.644	0.400	0.845
112	0.400	0.475	0.754
157	0.489	0.477	0.755
169	0.615	0.435	0.713
171	0.601	0.436	0.706
200	0.616	0.480	0.779

REFERENCES

- Allard, F., Hauschildt, P.H. 1995, *ApJ*, 445, 433
- Bessell, M.S. 1982, *Proc. ASA*, 4, 417
- Cohen, J.G., Hogg, D.W., Pahre, M.A., Blandford, R. 1996, *ApJ*, 462, L9
- Cohen, J.G. et al 1997, in preparation
- Cowie, L.L., Songaila, A., Hu, E.M., Cohen, J.G. 1996, *AJ*, 112, 839
- Gilmore, G., Reid, N. 1983, *MNRAS*, 202, 1025
- Gilmore, G.F., Wyse, R.F.G., Jones, J.B. 1995, *AJ*, 109, 1095
- Gizis, J.E. 1997, *AJ*, in press
- Landolt, A.U. 1992, *AJ*, 104, 340
- Larsen, J.A., Humphreys, R.M. 1996, *ApJ*, 468, L99
- Laureijs, R.J., Helou, G., Clark, F.O. 1994, in *First Symposium on the Infrared Cirrus and Diffuse Interstellar Clouds*, ASP Conf. Ser. 58, 133, ed. R. M. Cutri & W. B. Latter
- Majewski, S.R. 1992, *ApJS*, 78, 87
- Majewski, S.R. 1993, *ARA&A*, 31, 575
- Norris, J. 1987, *AJ*, 93, 616
- Oke, J.B. 1990, *AJ*, 99, 1621
- Ojha, D.K., Bienaymé, O., Robin, A.C., Crézé, M., Mohan, V. 1996, *A&A*, 311, 456
- Pahre, M.A. et al 1997, in preparation
- Reid, N., Majewski, S.R. 1993, *ApJ*, 409, 635 (RM93)
- Reid, I.N., Hawley, S.L., Gizis, J.E. 1995, *AJ*, 110, 1838 (RHG)
- Reid, I.N., Yan, L., Majewski, S.R., Thompson, I., Smail, I. 1996, *AJ*, 112, 1472 (RYMTS)
- Robin, A.C., Crézé, M., Mohan, V. 1992, *A&A*, 265, 32
- Robin, A.C. 1994, *IAU Symposium 161, Astronomy from Wide-field Imaging*, p. 403, ed. H.T. MacGillivray et al, Kluwer Academic Publishers, Dordrecht

Robin, A.C., Haywood, M., Crézé, M., Ojha, D.K., Bienaymé, O. 1996, *A&A*, 305, 125

Trefzger, Ch.F., Pel, J.W., Gabi, S. 1995, *A&A*, 304, 381

Wyse, R.F.G., Gilmore, G.F. 1988, *AJ*, 95, 1404

Yoss, K.M., Neese, C.L., Hartkopf, W.I. 1987, *AJ*, 94, 1600

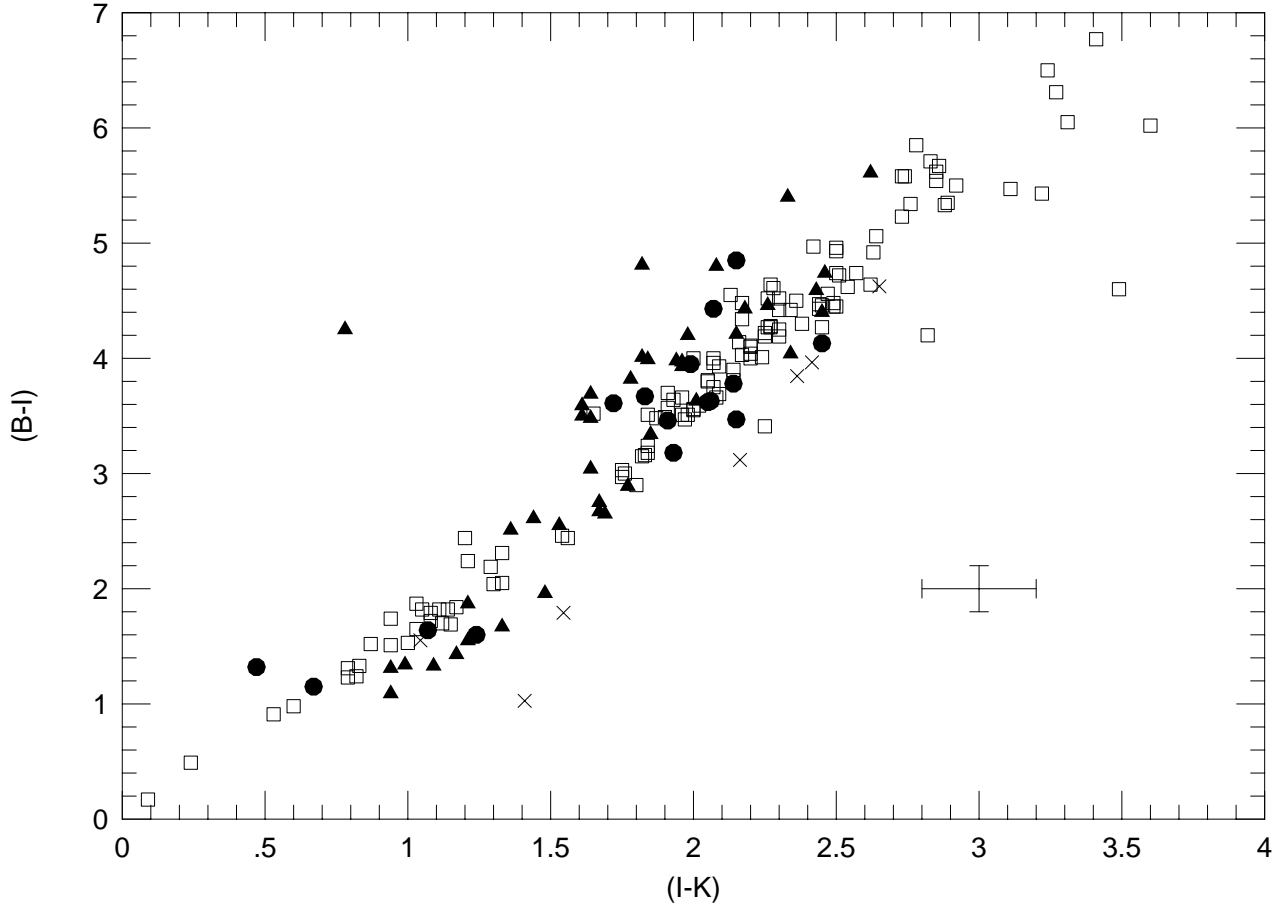


Fig. 1.— The $(B-I)/(I-K)$ two-colour diagram for stars in the 0-hour field (solid dots), SSA 13 (crosses) and SSA 22 (solid triangles). The reference sequence is provided by Leggett's (1992) photometry of stars within 8-parsecs of the Sun (plotted as open squares). The error-bar shows representative uncertainties for $I \sim 21$ magnitude and fainter.

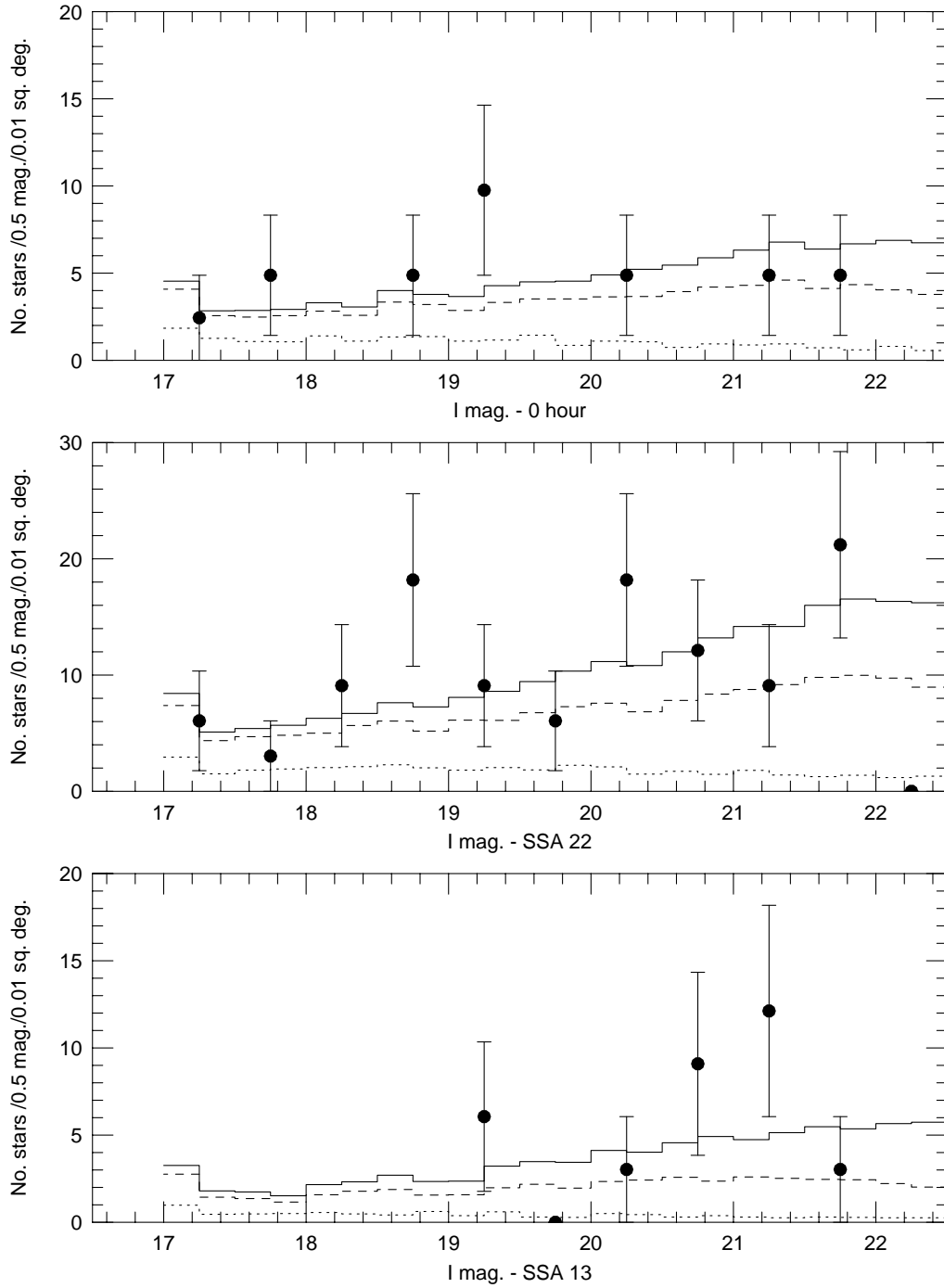


Fig. 2.— (a) Predicted and observed number counts for the three fields in this study. The solid histogram outlines the total counts; the dotted line marks the contribution of the old disk; and the dashed line separates the contribution from the IP II and halo.

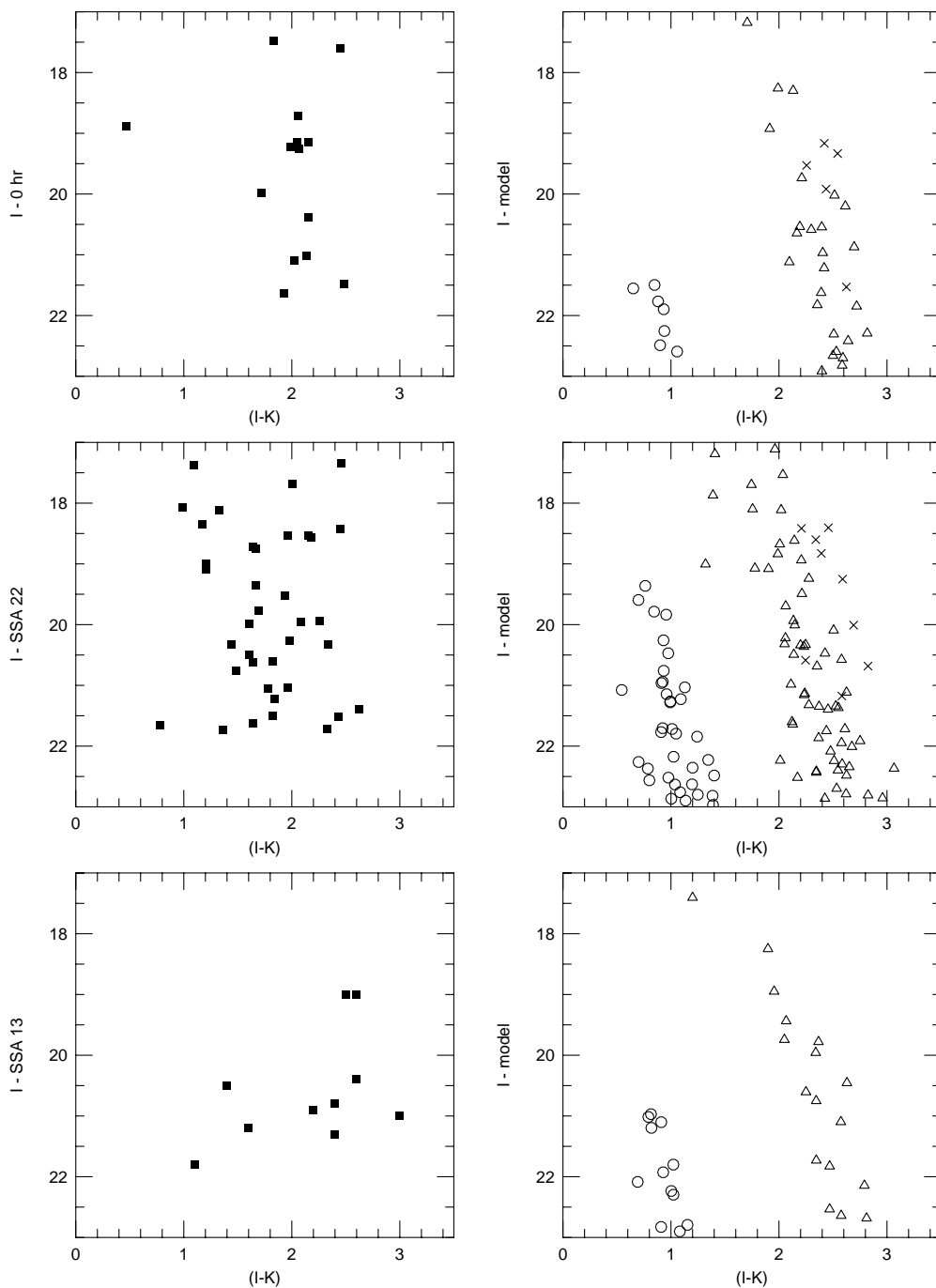


Fig. 2.— (b) Predicted and observed (I, I-K) colour magnitude diagrams. The right-hand panel show the predictions for each field (and for a solid angle of 0.01 square degrees) made by the model described in the text, where the red sequence is due to old disk (crosses) and IP II stars (triangles) and the blue due to halo stars (open circles). The left-hand panels plot the observed distributions.

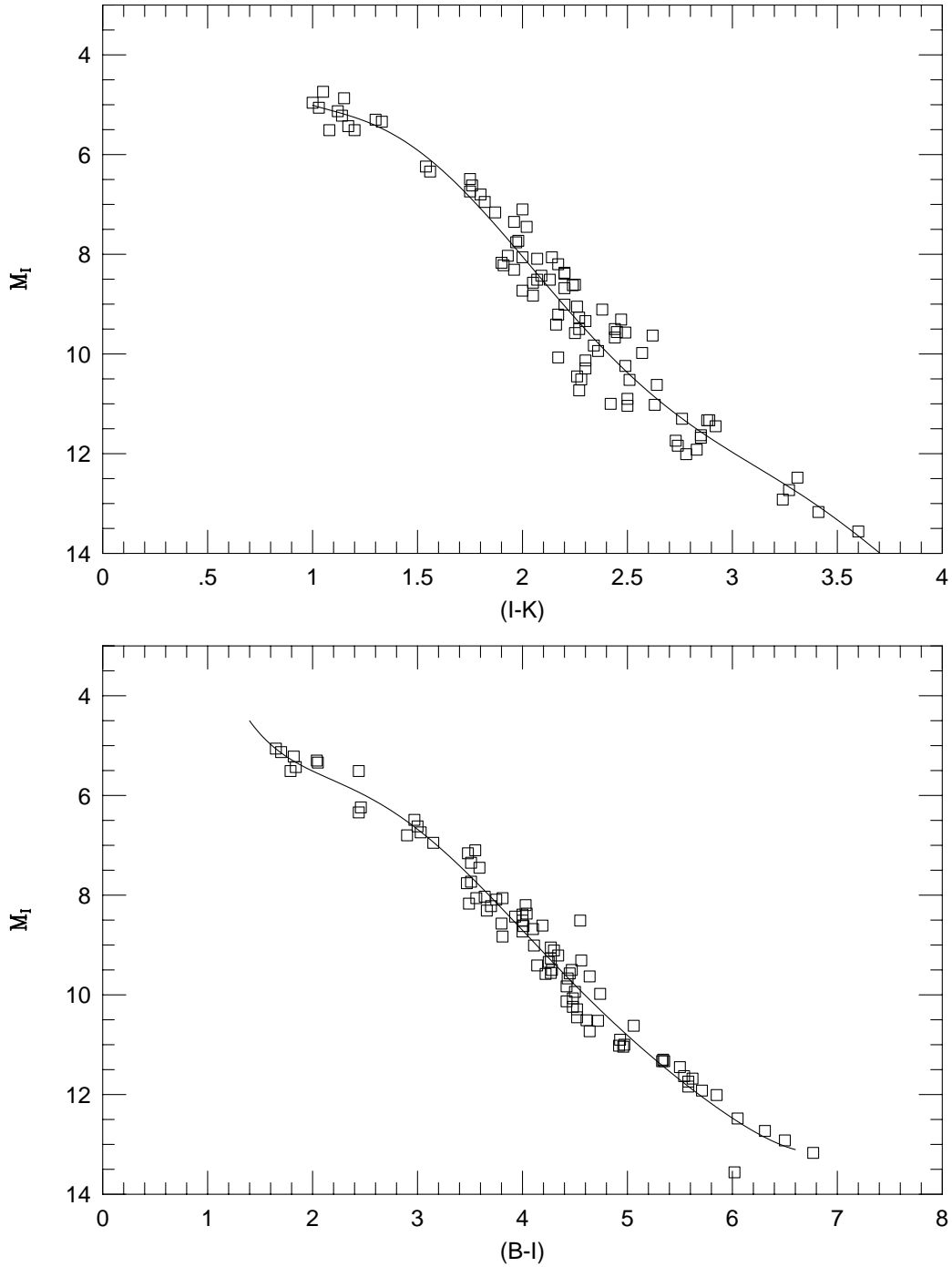


Fig. 3.— The $(M_I, (I-K))$ and $(M_I, (B-I))$ colour-magnitude diagrams defined by stars within 8-parscs of the Sun. The majority of the photometry is from Leggett (1992). In each case the line shows mean relation defined by a sixth order polynomial fitted to the data.

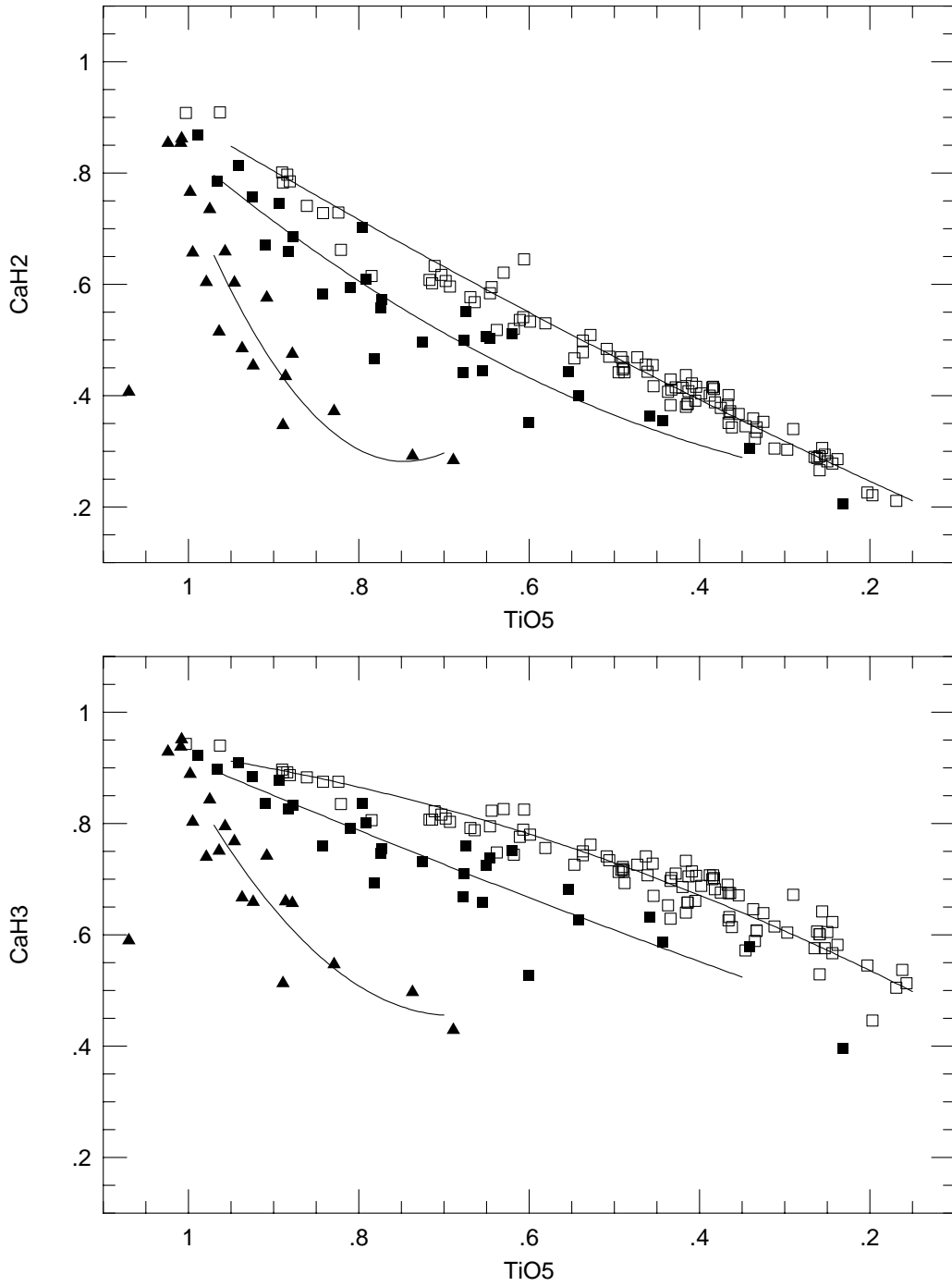


Fig. 4.— Calcium hydride strength as a function of the TiO $\gamma(0,0)$ bandstrength. Data for single stars within 8 parsecs of the Sun (from RHG) are plotted as open squares. These define a solar-abundance sequence. The solid symbols are subdwarfs from Gizis (1996), with the squares being ‘normal’ subdwarfs with $[\text{Fe}/\text{H}] \sim -1$ and the triangles ‘extreme’ subdwarfs, $[\text{Fe}/\text{H}] \sim -2$. Second-order polynomials fitted to each sequence are also shown.

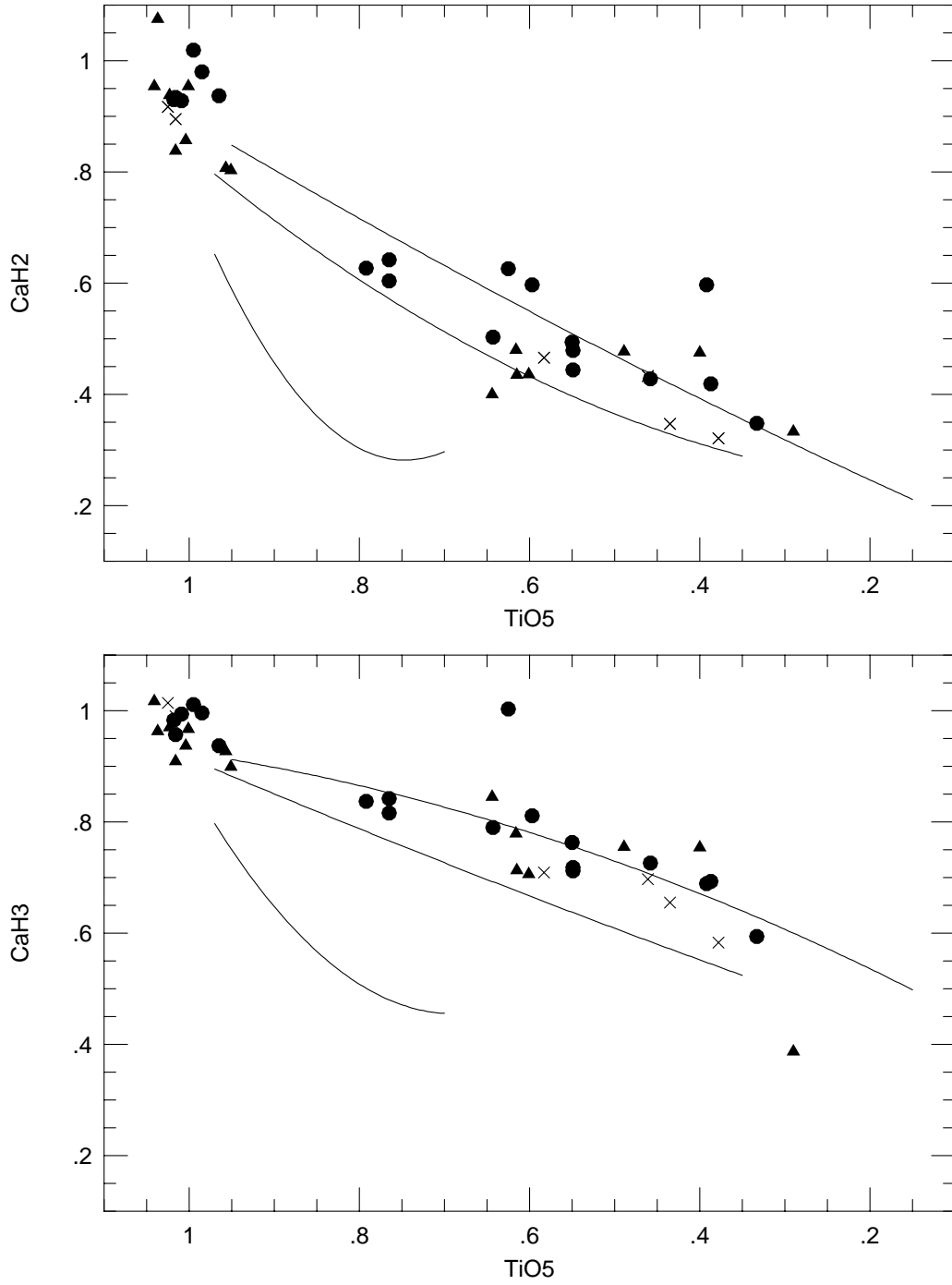


Fig. 5.— Calcium hydride and titanium oxide bandstrengths for the programme stars in our sample. The data are coded as in figure 1 and the fiducial lines are the polynomial fits to the disk dwarfs, intermediate subdwarfs and extreme subdwarfs from figure 4.

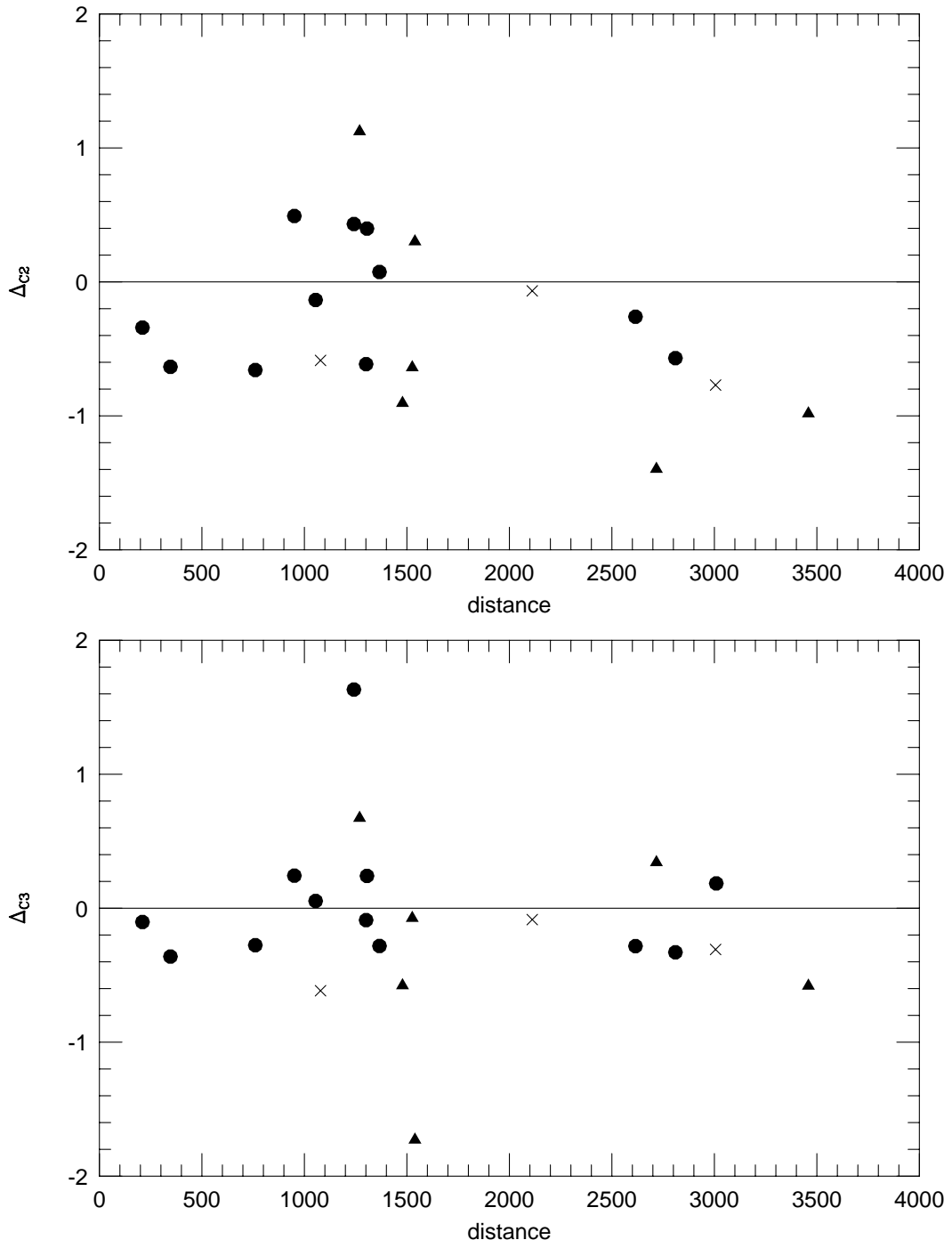


Fig. 6.— The normalised CaH indices, Δ_{C2} and Δ_{C3} plotted against distance above (or below) the Galactic Plane.